Table II. Q_{cc}'s and η's in Metavanadates

	Q_{cc}, kHz [η]		
	NMR (300 K)	NQR (300 K)	NQR (77 K)
KVO_3	4360 ± 60	4201 ± 2	4207 ± 2
	[0.75 ± 0.10]	[0.794 ± 0.001]	[0.877 ± 0.001]
$NaVO_3$	3650 ± 60	3745 ± 3	3725 ± 2
	[0.60 ± 0.10]	[0.489 ± 0.003]	[0.587 ± 0.001]
NH_4VO_3	2880 ± 60	2975 ± 20	2868 ± 5
	[0.30 ± 0.10]	[0.437 ± 0.020]	[0.363 ± 0.013]

highest frequency line could be missed because it is usually the easier one to detect. With these two lines as the two higher frequency responses, the quadrupole parameters are estimated to be Q_{cc} = 2868 ± 5 kHz and η = 0.363 ± 0.013. The third line is expected between 250 and 300 kHz. Attempts have been made to detect this line, but no obvious resonance was seen in the noisy spectra. It is believed that some modification of the Robinson oscillator must be made to reduce noises when operating below 300 kHz. The spectrum at 300 K was also taken. Only one line at 625 ± 1 kHz was detected with a decent signal-to-noise ratio. Two weak lines were found at 325 ± 5 and 400 ± 5 kHz. The quadrupole parameters would be 2975 ± 5 kHz for Q_{cc} and 0.437 ± 0.02 for η.

Table II lists the quadrupole interaction parameters of KVO_3, $NaVO_3$, and NH_4VO_3 obtained in this work. These metavanadates were previously studied by Baugher et al. using CW NMR and computer simulation techniques.[9] The results from that NMR study are also listed for comparison. Baugher also estimated the components of the chemical shift tensors in these compounds to be on the order of several hundred ppm. These fairly large chemical shift effects caused the calculation of the quadrupole interaction parameters to be not very accurate. It is clear that the quadrupole interaction parameters obtained through NQR and more than an order of magnitude more accurate than those obtained through NMR.

Conclusions

Pure ^{51}V NQR has been observed for KVO_3, $NaVO_3$, and NH_4VO_3 with decent signal-to-noise ratios (40 to 100 at 77 K and 6 to 8 at 300 K). The quadrupole interaction parameters obtained by this study are accurate to within 3 kHz for Q_{cc}'s and to within 0.001 for η's in most cases. These accurate quadrupole coupling parameters are useful not only in that they give structural information by themselves but also in that they can facilitate the analysis of NMR spectra. For example, knowing the exact quadrupole interaction parameters, it would be easier to extract chemical shift parameters from the NMR spectra for quadrupolar nuclei.

The line width of ^{51}V NQR lines from the metavanadates studied vary from 7 to 16 kHz. The narrow line widths indicate that ^{51}V NQR spectroscopy can resolve vanadium sites which differ in their NQR frequencies by 20 kHz or less. In the case of large η, multiquantum transitions can be observed. These lines can be used to ensure the correct calculation of the quadrupole parameters.

The sensitivity of the Robinson-type oscillator degrades when operating below 300 kHz. Some modification is necessary.

2D NOESY Simulations of Amide Protons in Acetamido Sugars†

Perseveranda Cagas, Kumaralal Kaluarachchi,‡ and C. Allen Bush*

Contribution from the Department of Chemistry and Biochemistry, University of Maryland Baltimore County, Baltimore, Maryland 21228. *Received January 11, 1991*

Abstract: Because of the flexibility of most small peptides, quantitative simulation of amide proton nuclear Overhauser effects (NOE) by relaxation matrix methods which ignore internal motion are not thought to be generally useful. But NOE simulations for the carbon-bound protons of some complex oligosaccharides carried out as a function of geometry have produced an excellent fit to experimental data suggesting that these carbohydrates adopt relatively rigid conformations. Therefore we have devised a method for simulation of amide proton NOE and applied it to the amide protons of GlcNAc in some Lewis blood group oligosaccharides which have been proposed to adopt rigid single conformations. The quantitative simulation of amide proton NOE is complicated by chemical exchange with solvent, by the effects of rapid quadrupolar relaxation of ^{14}N, and by dipolar relaxation of ^{14}N. The effects of chemical exchange can be eliminated by choice of solvent pH and temperature, and quadrupolar effects can be shown to be small for this case. The influence of ^{14}N dipolar relaxation is significant but can be readily calculated and incorporated into existing schemes for relaxation matrix computation of NOE in carbohydrates. NOESY spectra are reported in H_2O for two Lewis blood groups oligosaccharides, lacto-*N*-difucohexaose-1 and lacto-*N*-fucopentaose-1, with solvent suppression pulse sequences which have been used for peptides. Crosspeaks whose magnitudes depend on glycosidic dihedral angles are observed between the amide proton of GlcNAc and protons of the adjacent galactose residue. These values can be matched by simulations with the same model geometry deduced for these oligosaccharides from carbon-bound proton NOE supporting the rigid model hypothesis. Crosspeaks observed for the amide protons with protons in the same GlcNAc residue are sensitive to the orientation of the amide plane, and we propose slightly different dihedral angles for these two oligosaccharides. Vacuum ultraviolet circular dichroism spectra are reported on these human milk oligosaccharides which bear on the difference in the amide orientation in GlcNAc.

Introduction

Some workers who have studied the conformation of complex carbohydrates in solution have proposed that oligosaccharides, in contrast to small peptides which generally demonstrate a substantial amount of internal motion, assume relatively rigid conformations determined largely by steric repulsion.[1-3] In our research group, we have attempted to devise rigorous tests of this hypothesis as applied to a series of blood group oligosaccharides. Our primary experimental technique has been quantitative

† Research Supported by NIH Grant GM-31449.

‡ Present address: Department of Chemistry, Purdue University, West Lafayette, Indiana 47907.

* Author to whom correspondence should be addressed.

(1) Bush, C. A.; Cagas, P. In *Advances in Biophysical Chemistry*; Bush, C. A., Ed.; JAI Press: CT, in press.

(2) Bush, C. A.; Yan, Z.-Y.; Rao, B. N. N. *J. Am. Chem. Soc.* **1986**, *108*, 6168-6173.

(3) Rao, B. N. N.; Dua, V. K.; Bush, C. A. *Biopolymers* **1985**, *24*, 2207-2229.

0002-7863/91/1513-6815$02.50/0

measurements of the ^1H nuclear Overhauser effect (NOE) in NMR spectroscopy. For a number of tri- and tetrasaccharide fragments derived from the blood group H, blood group A, and Lewis blood group systems we have carried out complete spin matrix simulations under the assumption of a single isotropically rotating molecule.[2] We have generally found that variation of the geometry of the oligosaccharide, as parameterized through the glycosidic dihedral angles Φ and ψ, locates a single unique conformation or small group of closely related conformations consistent with our experimental NOE data.[4] Conformational energy calculations employing any of a number of widely used classical potential energy functions generally show that the conformations derived from the NOE data coincide with energy minima consistent with the hypothesis that these blood group oligosaccharides adopt single rigid conformations. Molecular dynamics simulations of these same oligosaccharides and the disaccharides of which they are made up show that, while the disaccharide constituents are often flexible, formation of the tri- or tetrasaccharide blood group fragment introduces steric repulsion effects which limit the conformations, greatly diminishing fluctuations in Φ and ψ, the glycosidic dihedral angles.[5]

The energy calculations indicate that the major effect in determining the minimum energy conformations of these oligosaccharides is steric repulsion between closely packed atoms. As an experimental test of this prediction of the modeling calculations, NOE data on some of the blood group oligosaccharides have been recorded as a function of temperature. We find that NOE data over a range of temperature can be simulated with the same oligosaccharide model indicating the absence of any thermal melting such as that seen in peptides, proteins, and oligosaccharides.[3,6] Circular dichroism (CD) data for certain oligosaccharides as a function of temperature are also consistent with this interpretation.[3] As a further test of the hypothesis that steric repulsions dominate in determining the conformation of blood group oligosaccharides, NOE data on these oligosaccharides have been recorded in such varied solvents as D_2O, pyridine, and Me_2SO. The results of these studies have shown that the same oligosaccharide model fits the NOE data for all three solvents suggesting that no solvent denaturation occurs, a result which we interpret as consistent with the dominance of steric effects over hydrogen bonding or hydrophobic effects in stabilizing the conformation.[7]

^{13}C relaxation measurements can be used as a direct measure of internal motion in oligosaccharides. While technical difficulties have limited the range of complex oligosaccharides to which this method has been applied, ^{13}C T_1 data have been reported for some oligosaccharides carrying the Lewis blood group determinants isolated from human milk.[8] These preliminary results recorded at a single magnetic field strength have been interpreted as showing little internal motion. ^{13}C T_1 data have been reported for mucin glycoproteins carrying blood group A oligosaccharides which are consistent with a relatively rigid blood group determinant.[9]

We should point out that not all workers who have studied carbohydrate conformation agree with the rigid model. Some data on biologically interesting carbohydrates provide rather convincing evidence for internal motion. Scarsdale et al.[10] argue that the core tetrasaccharide of gangliosides can adopt several different conformations depending on the substitution pattern of the NeuNAc residues. Glaudemans et al.[11] present evidence that the disaccharide Galβ(1→6)Gal adopts a distribution of conformations which is modified on binding to a specific monoclonal antibody. Carver and Cumming[12] have carried out a careful analysis of NOE and coupling constants related to the conformation of the Manα(1→6)Man and the Manα(1→3)Man linkage in asparagine N-linked glycopeptides of glycoproteins which argues for an average of conformations. It is our interpretation that the evidence for internal motion in complex oligosaccharides does not invalidate our conclusions regarding the rigid conformations adopted by the blood group structures. We suggest that different oligosaccharides have different conformational properties and that the ability to distinguish between rigid and flexible structures could be valuable to our understanding of the biological function of complex carbohydrates. Therefore we propose that new spectroscopic methods be employed to further test and refine the hypothesis of rigid oligosaccharide conformations and to discriminate structures which have internal motion from those which do not.

This report concerns the measurement and the quantitative interpretation of the NOE of the amide protons of *N*-acetyl amino sugars in complex oligosaccharides. While the exchange of these protons with solvent in aqueous media presents technical difficulties in the measurement, experience in peptide and protein chemistry provides powerful techniques adequate to overcome these problems. We also present a method for the quantitative interpretation of the amide proton NOESY data by a full spin matrix approach which is a slight modification of our recently published method for carbon-bound protons. This method is applied to Lewis blood group oligosaccharides resulting in new information on the glycosidic dihedral angles Φ and ψ as well as some insight into the orientation of amide plane. CD data are also reported which bear on the amide dihedral angle.

Materials and Methods

Sample Preparation. A mixture of oligosaccharides was isolated from human milk following the method of Kobata and Ginsburg[13] and Kobata et al.[14] The oligosaccharides lacto-*N*-difucohexaoase 1 (LND-1) [Fucα(1→2)Galβ(1→3)[Fucα(1→4)]GlcNAcβ(1→3)Galβ(1→4)Glc] and lacto-*N*-fucopentaose 1 (LNF-1) [Fucα(1→2)Galβ(1→3)-GlcNAcβ(1→3)Galβ(1→4)Glc] were prepared from this mixture by Bio-Gel P6 filtration followed by reverse-phase high-performance liquid chromatography of the gel fractions.[15] For NMR spectroscopy, samples in D_2O were prepared by dissolving 5–7 mg of oligosaccharide in D_2O and lyophilizing for three cycles, making up the final solution with 450 μL of high-purity D_2O (99.96 atom %, Merck, Sharp & Dohme). Samples in H_2O were prepared by dissolving oligosaccharides in 450 μL of a mixture (pH 2.3) of 90% H_2O/10% D_2O with trifluoroacetic acid.

NMR Spectroscopy. Phase-sensitive 2D NOESY experiments were conducted at 500 MHz on a GN-500 spectrometer at 5 °C and 250 ms mixing time with the method of States et al.[16] Experiments in D_2O utilized the standard NOESY pulse sequence.[17] For observation of labile acetamido protons, a spin-echo type of water suppression was used.[18] In this scheme, the final 90° pulse of the standard NOESY sequence is replaced by a composite pulse consisting of a 1-1 ($90°_x$–τ_1–$90°_{-x}$) hard pulse followed by a 1-1 ($90°_x$–τ_2–$90°_{-x}$) refocusing pulse. The delays τ_1 and τ_2 (139 and 278 μs, respectively) were chosen to yield maximum excitation at the NH resonance. Weak decoupler presaturation of the water signal was employed during the recycle delay period (2.5 s), and a 10 ms homospoil pulse was applied during the mixing period to remove transverse water magnetization before the echo sequence.

Data size was 256 points in t_1 and 1024–2048 points in t_2. Raw data were transferred from the GN 500 spectrometer via an ethernet link to either a VAXstation 3200 or Silicon Graphics 4D/20 for offline processing with FTNMR software (Hare Research, Woodinville, WA). The free induction decays were multiplied by 90° shifted sine bell functions before Fourier transformation in each dimension. Further experimental details are found in the figure captions.

(4) Cagas, P.; Bush, C. A. *Biopolymers* **1990**, *30*, 1123–1138.
(5) Yan, Z.-Y.; Bush, C. A. *Biopolymers* **1990**, *29*, 799–812.
(6) Rao, B. N. N.; Bush, C. A. *Carbohydr. Res.* **1988**, *180*, 111–128.
(7) Yan, Z.-Y.; Rao, B. N. N.; Bush, C. A. *J. Am. Chem. Soc.* **1987**, *109*, 7663–7669.
(8) Bush, C. A.; Panitch, M. M.; Dua, V. K.; Rohr, T. E. *Anal. Biochem.* **1985**, *145*, 124–136.
(9) Gerken, T. A.; Butenhof, K. J.; Shogren, R. *Biochemistry* **1989**, *28*, 5536–5549.
(10) Scarsdale, J. N.; Prestegard, J. N.; Yu, R. K. *Biochemistry* **1990**, *29*, 9843–9855.
(11) Glaudemans, C. P. J.; Lerner, L.; Daves, G. D.; Kovac, P.; Venable, R.; Bax, A. *Biochemistry*, **1990**, *29*, 10906–10911.
(12) Carver, J. P.; Cumming, D. A. *Pure Appl. Chem.* **1987**, *59*, 1465–1467.
(13) Kobata, A.; Ginsburg, V. *J. Biol. Chem.* **1969**, *244*, 5496–5502.
(14) Kobata, A.; Tsuda, M.; Ginsburg, V. *Arch. Biochem. Biophys.* **1969**, *130*, 509–513.
(15) Dua, V. K.; Bush, C. A. *Anal. Biochem.* **1983**, *133*, 1–8.
(16) States, D. J.; Hakerborn, R. A.; Ruben, D. J. *J. Magn. Reson.* **1982**, *48*, 286–292.
(17) Kumar, A.; Wagner, G.; Ernst, R. R.; Wuthrich, K. *J. Am. Chem. Soc.* **1981**, *103*, 3654–3658.
(18) Sklenar, V.; Bax, A. *J. Magn. Reson.* **1987**, *74*, 469–479.

Saturation transfer experiments were performed by obtaining one-dimensional spectra in water with and without decoupler presaturation (3s) of the water signal. The NH proton intensities were then integrated and compared.

Selective spin-lattice relaxation rates of NH protons were measured with the decoupler for selective inversion followed by a variable delay and a 1-1 echo read pulse. T_1's were obtained by fitting the data to a single exponential.

Measurement of NOE Intensities and NOESY Simulation. Nuclear Overhauser effects were integrated by summing over all points in the rows and columns in the spectra which contain a particular crosspeak. This procedure was applicable both for ordinary NOESY data on carbon-bound protons and for the amide protons in water-suppressed spectra since the relative intensities of signals in slices taken parallel to the F_1 dimension are unaffected by the 1-1 echo pulse as will be discussed below. NOESY crosspeak intensities were normalized by the intensity of a single proton at zero mixing time. The latter was obtained from the intensity of an isolated diagonal peak extrapolated to zero mixing time with the measured selective T_1 of that peak.[4] To avoid the complication of nonuniform excitation in F_2 by the 1-1 water suppression pulse, the diagonal peak for normalization of amide proton crosspeaks was always chosen from the same column. While this is not always possible for the strongly overlapping resonances of carbon-bound protons of carbohydrates, it does not present a problem for the amide proton resonances which are generally well isolated in the spectrum. The experimental error limits were determined from the noise level in the spectrum and errors in choosing the size of the integration region, as explained previously.[4]

Three-dimensional models necessary for the simulation of the NOESY data were constructed from monosaccharide X-ray crystallographic data,[19,20] with each monosaccharide unit fixed in the $^4C_1$ (GlcNAc, Gal) or $^1C_4$ (Fuc) conformation. The glycosidic angle was fixed at 117°, and the conformation varied by changing the glycosidic dihedral angles. Simulation of NOEs from nonexchangeable protons of LNF-1 was performed with the procedure of Cagas and Bush.[4] Disaccharide models for the linkages Fucα(1→2)Gal and Galβ(1→3)GlcNAc were constructed, and the conformations searched in 10° intervals of the glycosidic dihedral angles. Disaccharide conformations whose calculated NOEs across each glycosidic bond agreed with their experimental values were determined. To facilitate comparison of the computed with the experimental NOE, ratios of interresidue NOE to intraresidue NOE were calculated and compared with experimental values. The following ratios of NOE intensities were used: Fuc^2 H1/Gal^3 H2 to Fuc^2 H1/H2, Gal^3 H1/GlcNAc H3 to Gal^3 H1/H3, and Fuc^2 H5/GlcNAc H2 to GlcNAc H1/H3. A trisaccharide model Fucα(1→2)Galβ(1→3)GlcNAcβOMe was then used to search among these disaccharide conformations for trisaccharide conformations with calculated NOEs consistent both with experimental crosspeak intensities between protons located directly across a glycosidic linkage and those between protons on nonadjacent residues.

Simulation of NOESY intensities from NH protons was done with the same general procedure for carbon-bound protons described above. As will be explained in detail under Discussion, it was necessary to modify the simulation by inclusion of a term in the calculated ^{1}H spin-lattice relaxation rate representing the contribution of directly bonded ^{14}N to the dipolar relaxation of the amide proton, in addition to the usual contributions from other protons in the molecule. The relaxation rate matrix for all protons in the system was calculated under the assumption of a single correlation time τ_c which was adjusted to reproduce an intraresidue NOE, with data on carbon-bound protons in D_2O. The matrices of eigenvectors and eigenvalues obtained from diagonalization of the relaxation rate matrix were then used to calculate theoretical NOESY peak intensities as a function of the mixing time.[21,22]

For NOESY intensity matrices for model conformations, the trisaccharide fragment Fucα(1→2)Galβ(1→3)GlcNAcβOMe was employed for LNF-1 and the tetrasaccharide fragment Fucα(1→2)Galβ-(1→3)[Fucα(1→4)]GlcNAcβOMe was used for LND-1. NOESY crosspeak intensities were calculated as a function of the amide dihedral angle τ, defined by the atoms C_1-C_2-N-C, and the glycosidic dihedral angles Φ and ψ, defined by atoms O_τ-C_1-O_1-C_x and C_1-O_1-C_x-C_{x-1}, respectively. In the conformational search, the amide dihedral angle was varied in 10° steps from 0 to 360°, while the glycosidic dihedral angles were searched also in 10° steps and within ±30° of the values which were previously found to agree with experimental NOESY and T_1 data for carbon-bound protons in D_2O. In the simulation procedure, NOE intensities from both exchangeable and nonexchangeable protons were calculated, their ratios to an intraresidue NOE determined and compared with experimental ratios. For both oligosaccharides, the intraresidue NOE used to calculate NOE ratios was the GlcNAc H1/H3 NOE intensity which was obtained from data in D_2O.

Circular Dichroism Measurements. CD measurements were made on a home-made instrument having a vacuum monochromator and the sample at atmospheric pressure in a nitrogen purged sample chamber.[23] Spectra in the wavelength region from 170 to 230 nm were multiply scanned and signal averaged and smoothed by Fourier digital filtering.[24] Since these oligosaccharides contain the amide as the only chromophore which absorbs light in the above wavelength range, absorbance of this chromophore at 190 nm was used to determine the concentration taking $\epsilon = 9000$.[25] Spectra were recorded in D_2O with 1- and 0.1-mm quartz cells with a correction for the solvent baseline by digital subtraction.

Results

^{1}H assignments for both LNF-1[3] and LND-1[26] in D_2O have been previously made at 24 °C, and the chemical shifts at 5 °C were found to be within ±0.01 ppm of the values at 24 °C. For the exchangeable NH protons of the GlcNAc residue the chemical shifts with respect to acetone at 2.225 ppm measured at 5 °C were 8.605 ppm (J = 10.1 Hz) for LND-1 and 8.566 ppm (J = 10.2 Hz) for LNF-1. Since chemical exchange of amide protons with solvent can influence the NOESY crosspeak intensities under conditions for which the exchange rate is comparable to $1/T_1$, saturation-transfer experiments were used to determine the effect of chemical exchange with solvent on the NH intensities. Under our experimental conditions of pH and temperature, signals showed negligible (<1%) loss of intensity upon water presaturation.

A contour plot of the NOESY spectrum of LNF-1 in D_2O at 5 °C and 250 ms mixing time is given in Figure 1, showing crosspeaks from nonexchangeable protons. Crosspeaks from the anomeric protons to protons across the glycosidic linkage are observed between Fuc^2 H1 and Gal^3 H2, Gal^3 H1 and GlcNAc H3, GlcNAc H1 and Gal^4 H3, and Gal^4 H1 and β-Glc H4. An NOE involving nonadjacent residues is also observed, between Fuc^2 H5 and GlcNAc H2. In addition to these interresidue NOEs several effects within the individual monosaccharide units are also seen. The experimental normalized NOE intensities of these peaks along with the error limits are shown in Table I. A contour plot and cross section through the amide resonance of the NOESY spectrum in water of LNF-1 at a mixing time of 250 ms and at 5 °C (Figure 2) show crosspeaks from the amide proton of GlcNAc to H1 of Gal^3 and to protons within the GlcNAc unit, H2, H3 and to the methyl group of the acetamido side chain. Quantitative interpretation of the crosspeak involving the methyl group was not included in our simulation procedure because of complications introduced by internal rotation. An approximate treatment[27,28] for incorporating methyl group interactions is useful only under extreme narrowing, a situation which does not hold in the case of LNF-1 and LND-1 at 5 °C.

From the NOESY experiment in water for the hexasaccharide, LND-1, a contour plot of the amide region and an F_1 cross section through the amide resonance (Figure 3) reveals crosspeaks from the exchangeable NH proton of GlcNAc to H1 of the adjacent Gal^3 residue and to protons within the GlcNAc residue. NH crosspeaks are detected for GlcNAc H2, H3 and the methyl group of the acetamido side chain as well as for GlcNAc H1, a peak which is absent in the NOESY spectrum of LNF-1 (see Figure 2) suggesting that there may be some difference between the amide orientation angles τ in the two oligosaccharides. Table II lists

(19) Longchambon, P. F.; Ohannessian, J.; Avenel, D.; Neuman, A. *Acta Crystallogr. B* **1975**, *31*, 2623-2627.
(20) Arnott, S.; Scott, W. E. *J. Chem. Soc., Perkin Trans. 2* **1971**, 324-335.
(21) Keepers, J. W.; James, T. L. *J. Magn. Reson.* **1984**, *57*, 404-426.
(22) Borgias, B. A.; Gochin, M.; Kerwood, D. J.; James, T. L. *Prog. NMR Spectrosc.* **1990**, *22*, 83-100.
(23) Duben, A. J.; Bush, C. A. *Anal. Chem.* **1980**, *52*, 635-638.
(24) Bush, C. A.; Ralapati, S.; Duben, A. J. *Anal. Chem.* **1981**, *46*, 890-895.
(25) Coduti, P. L.; Gordon, E. C.; Bush, C. A. *Anal. Biochem.* **1977**, *78*, 9-20.
(26) Breg, J.; Romijn, D.; Vliegenthart, J. F. G.; Strecker, G.; Montreuil, J. *Carbohydr. Res.* **1988**, *183*, 19-24.
(27) Woessner, D. E.; Snowden, B. S., Jr.; Meyer, G. H. *J. Chem. Phys.* **1969**, *50*, 719-721.
(28) Heatley, F.; Akhter, L.; Brown, R. T. *J. Chem. Soc., Perkin Trans. II* **1980**, 919-924.

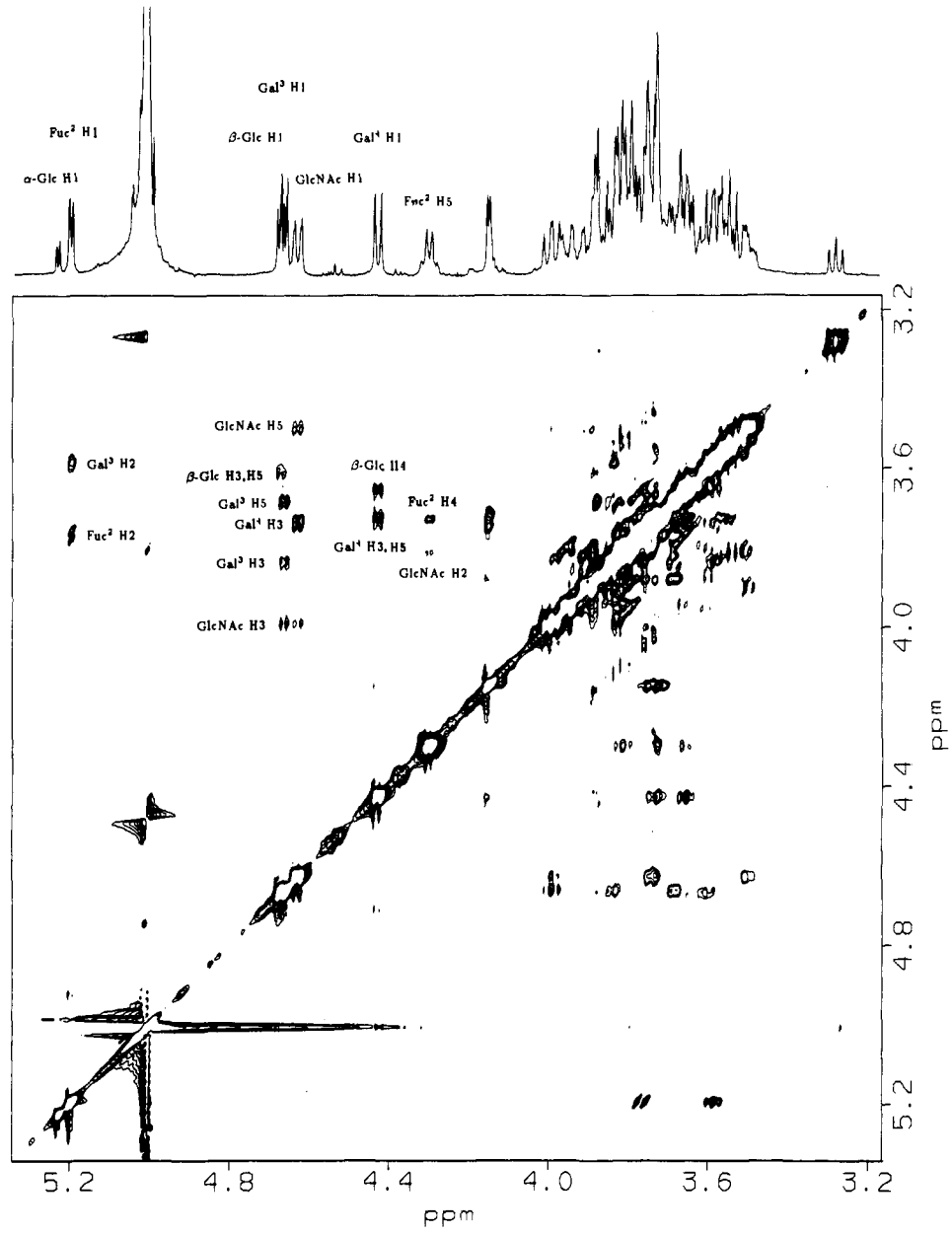

Figure 1. The 500 MHz ^{1}H NOESY spectrum of LNF-1 in D_2O, 5 °C, mixing time = 250 ms. Spectral width was ±1171 Hz, and raw data size was 2 × 256 × 1024 complex points with 32 transients per t_1 value.

the experimental normalized NOE intensities from the amide protons for both LNF-1 and LND-1. NOESY and T_1 data for LND-1 in D_2O and in DMSO-d_6/D_2O have been previously reported and the glycosidic angles ψ and Φ for the Fucα(1→2)Gal, Galβ(1→3)GlcNAc and Fucα(1→4)GlcNAc linkages in LND-1 have been determined.[4]

Simulations of the NOESY spectra as a function of the conformation of the nonreducing terminal blood group fragments were carried out for comparison with the data reported above for LNF-1 and LND-1. The orientation of the amide side chain was determined in both LNF-1 and LND-1 by variation of the amide angle τ and of the glycosidic ψ and Φ angles with the modified procedure described in Methods. A list of model tri- and tetrasaccharide conformations for LNF-1 and LND-1 whose calculated NOE ratios were found to agree with their experimental values within the error limits specified in Tables I and II is given in Table III. The values of the glycosidic dihedral angles ψ and Φ determined in this simulation are consistent with those previously obtained for both LNF-1[3] and LND-1[4] with only nonexchangeable proton NOEs. Furthermore, small differences of ≈10° are observed in the values of the ψ and Φ angles for the same linkages in the two sugars, although it is also noted that the range of values for the amide angle τ in the two differ by ≈30°. There is also a wider range of values for the amide angle τ − 90 ± 20 for the LND-1 tetrasaccharide and 60 ± 30 for the LNF-1 trisaccharide model.

Table 1. Experimental Nuclear Overhauser Enhancements for Nonlabile Protons, LNF-1 at 250 ms Mixing Time, 5 °C

crosspeak	% NOE[a]	crosspeak	% NOE[a]
Fuc²H1-Gal³ H2[b]	3 (±1)	GlcNAc H1-H3*	3 (±1)
Fuc² H1-H2*	3 (±1)	GlcNAc H1-H5	5 (±1)
Gal³ H1-GlcNAc H3	4 (±1)	Fuc² H5-GlcNAc H2	6 (±2)
Gal³ H1-H5	3 (±1)	Fuc² H5-H4	3 (±1)
Gal³ H1-H3*	3 (±1)	Fuc² H5-H3[c]	2 (±1)

[a] 100 × (crosspeak intensity at t_m = 250 ms/(diagonal peak intensity of a single proton at t_m = 0 ms). Intensities at t_m = 0 were obtained from T_{1sel} of diagonal peaks. Numbers in parentheses refer to experimental error limits. Crosspeaks marked with an asterisk are intraresidue NOEs used to calculate NOE ratios. [b] A superscript at the name of a sugar residue indicates to which position of the adjacent monosaccharide it is glycosidically linked, e.g., Gal³ means Gal is β(1→3)-linked to GlcNAc. [c] Cross peak can be observed at a contour level lower than that used in Figure 1.

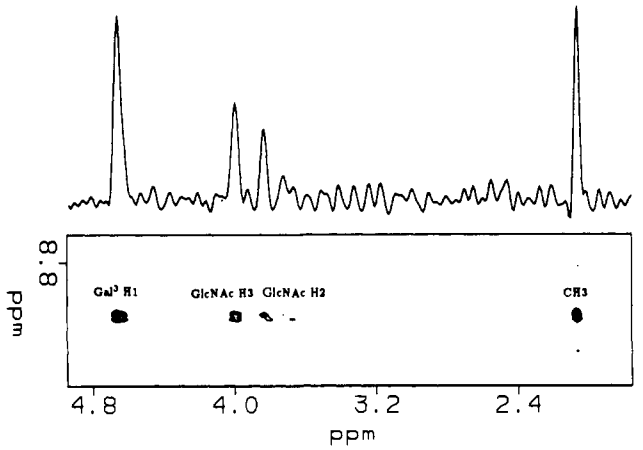

Figure 2. Contour plot and a column cross section through the amide region of the 500 MHz NOESY spectrum of LNF-1 in 90% H_2O/10% D_2O with 0.01 M trifluoroacetic acid. Temperature was 5 °C and a mixing time of 250 ms was used. Spectral width was ±2304 Hz, and τ_1 and τ_2 delays of 139 and 278 μs, respectively, were used in the water suppression scheme (see text). Raw data size was 2 × 256 × 2048 complex points, with 64 transients per t_1 value.

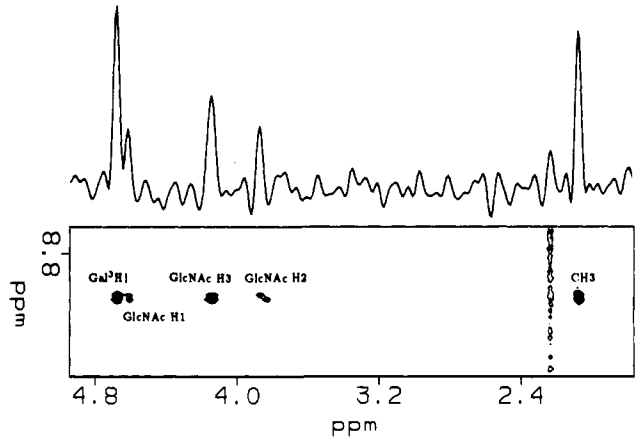

Figure 3. Contour plot and a column cross section through the amide region of the 500 MHz NOESY spectrum of LND-1 in 90% H_2O/10% D_2O with 0.01 M trifluoroacetic acid. A 250 ms mixing time and temperature of 5 °C were used. Sweep width was ±2304 Hz, and τ_1 and τ_2 delays of 139 and 278 μs, respectively, were used. Raw data size was 2 × 256 × 2048 complex points, and 64 transients per t_1 value were acquired.

Circular dichroism data in the wavelength region of the amide chromophore are given in Figure 4 for LND-1 and LNF-1 as well as for lacto-*N*-tetraose (LNT), the unfucosylated core tetrasaccharide common to both oligosaccharides. CD bands in this wavelength region are assigned to the amide n–π* transition at 209 nm and to the amide π–π* transition at 188 nm. It has been previously pointed out that the CD bands for LNF-1 are much larger than those for LNT and the interpretation of this result is that the Fuc[2] residue, which is tightly folded near the GlcNAc amide chromophore in the models based on NOE data, provides an asymmetric perturbation of the chromophore inducing the larger rotational strengths.[3] The previously published stereopairs representing the models for LNF-1[3] and for LND-1[4], which are consistent within experimental error with the present NMR data, illustrate this feature quite well. The surprising result in Figure 4 is that the CD spectrum of LND-1, which according to our interpretation of the NMR data has a folded conformation similar to that of LNF-1, has bands much smaller than those of the pentasaccharide and more similar to those of LNT. Our interpretation of the NOESY data is that the differences in conformation between LNF-1 and LND-1 must be very subtle and the additional fucose residue (Fuc[4]) in the latter oligosaccharide is on the opposite side of the model, quite remote from the amide chromophore in a location where it is unlikely to exert a direct influence on the CD bands from the amide. Also included in Figure 4 are CD data for the Lewis[a] pentasaccharide LNF-2, Galβ(1→3)[Fucα(1→4)]GlcNAcβ(1→3)Galβ(1→4)Glc. This spectrum resembles that of the parent tetrasaccharide, LNT, from which it differs by the addition of Fuc[4] which is located far from the amide chromophore in our model based on NOE data.[4]

Table II. Experimental NH Nuclear Overhauser Enhancements for LNF-1 and LND-1 at 250 ms and 5 °C

	% NOE[a]	
crosspeak	LNF-1	LND-1
NH-Gal³ H1	4 (±1)	4 (±1)
NH-GlcNAc H1		2 (±1)
NH-GlcNAc H2	<1	1.5 (±1)
NH-GlcNAc H3	2 (±1)	3 (±1)
NH-CH_3	3 (±1)	4 (±1)

[a] 100 × (crosspeak intensity at t_m = 250 ms/(diagonal peak intensity of a single proton at t_m = 0 ms). Intensities at t_m = 0 were obtained from T_{1sel} of NH (386 ± 17 and 348 ± 28 ms for LNF-1 and LND-1, respectively). Error limits are give in parentheses. Intraresidue NOE crosspeak used to calculate NOE ratios was GlcNAc H1/H3.

Calculations of the rotational strength of the amide n–π* transitions of 2-acetamido sugars have shown that the rotational strength is extremely sensitive to small changes in geometry.[29] A change of as little as 30° in the dihedral angle describing the orientation of the amide can change the rotational strength by a factor of 2. Such a difference in the orientation of the amide chromophore between LND-1 and LNF-1 would not be inconsistent with our NOE data, and the differences in the relative intensities of the amide proton crosspeaks to GlcNAc H1 and H3 suggest that such a subtle difference in amide orientation could indeed be present. Whether such a modest difference in conformation could have any biological significance, such as in binding of these Lewis active blood group oligosaccharides to antibodies and to lectins, remains to be determined. Our interpretation of the amide NMR data and the CD spectra indicates that such differences should be considered.

Discussion

Although one-dimensional steady-state NOEs have been reported previously for LNF-1 in D_2O, quantitative interpretation of the data was complicated by overlapping of resonances. Specifically signals of β-Glc H1, GlcNAc H1 and Gal³ H1 all resonate within 20 Hz making selective irradiation, which is in practice about 50–100 Hz wide, difficult or impossible. The added resolution introduced by the second dimension in the NOESY experiment eliminates problems of spillover encountered in selective inverting or saturating pulses. Thus, it was possible to make quantitative measurements of most of the NOEs useful in defining the glycosidic ψ and Φ angles.

The NOESY spectrum in D_2O for LNF-1 (Figure 1) shows crosspeaks from the carbon-bound protons whose intensities (Table I) were used to determine glycosidic dihedral angles ψ and Φ for each of the linkages Fucα(1→2)Gal and Galβ(1→3)GlcNAc. The ψ and Φ values obtained with a trisaccharide model (Table III) were similar to those reported by Rao et al.[3] with 1-D difference NOE spectroscopy. Simulation of the relatively large (6%) remote NOE between Fuc[2] H5 and GlcNAc H2 and the other two interglycosidic NOEs indicates a conformation for the LNF-1 trisaccharide in which the fucose ring is folded over to the GlcNAc residue, as was found in LND-1.[4] It is important to note that the presence of remote NOEs, in this case between Fuc[2] H5 and GlcNAc H2, is critical in reducing the number of possible conformations since these NOEs depend on more than one glycosidic linkage. This has been observed in all the blood group oligosaccharides we have studied so far.[2,4,7]

Since quantitative interpretations of amide NH NOESY data by spin matrix methods are not commonly found in the literature on either sugars or peptides, we should discuss some of the salient

(29) Yeh, C.-Y.; Bush, C. A. *J. Phys. Chem.* **1974**, *78*, 1829–1833.

Table III. LND-1 and LNF-1 Model Conformations Consistent with Experimental NOE[a] from Exchangeable and Nonexchangeable Protons

τ	Φ_{Gal}	Ψ_{Gal}	Φ_{Fuc^2}	Ψ_{Fuc^2}	Φ_{Fuc^4}	Ψ_{Fuc^4}
A. LND-1 Tetrasaccharide: Fucα(1→2)Galβ(1→3)[Fucα(1→4)]GlcNAcβOMe						
90 (±20)	−70 (±10)	−100 (±10)	−80 (±10)	140 (±10)	−70 (±10)	140 (±10)
B. LNF-1 Trisaccharide: Fucα(1→2)Galβ(1→3)GlcNAcβOMe						
60 (±30)	−80 (±10)	−110 (±10)	−70 (±10)	130 (±10)		

[a] Refer to Tables I and II for experimental NOEs.

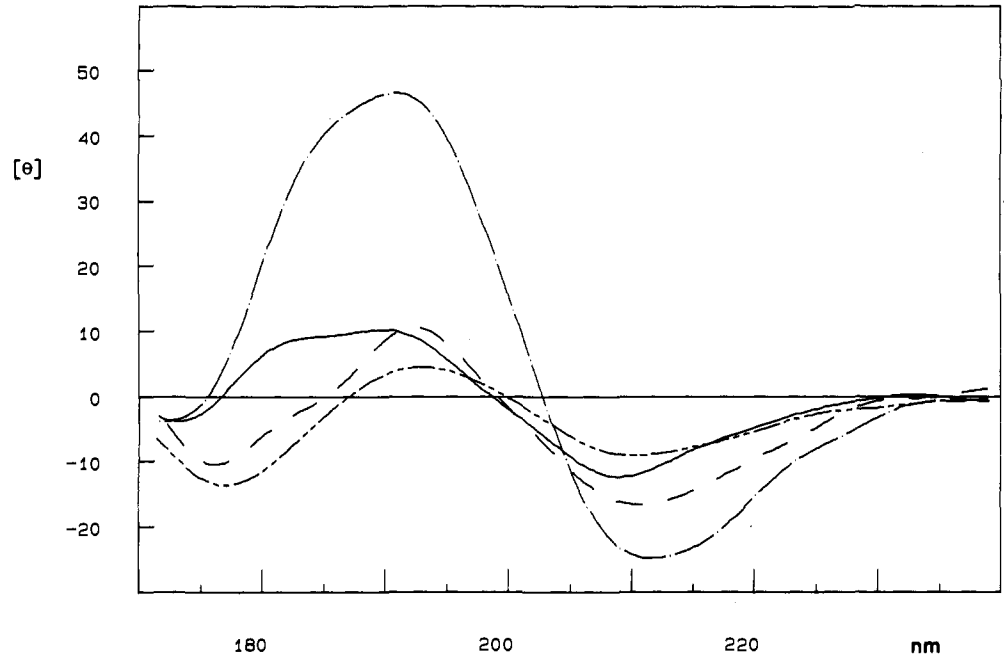

Figure 4. CD spectra of LNF-1 (-•-), LND-1 (—), LNF-2 (--) and LNT (----) at 25 °C. Wavelength is in nanometers and CD units are molar ellipticity $[\theta] \times 10^{-3}$.

features which are not encountered in interpretation of NOESY data for carbon-bound protons. First, one must consider the chemical exchange of NH protons with solvent. Our saturation-transfer data support the assumption that the rate of chemical exchange of the amide proton with solvent (H_2O) is sufficiently slow under the acidic conditions (pH ≈ 2.3) used so that the amide NOE intensities are essentially unaffected. Previous studies[30] with a dodecapeptide have shown that a minimum in the exchange rate of the amide proton occurs at pH ≈ 2.3. Studies of the amide proton exchange rates of the GlcNAc unit of group A streptococcal polysaccharide and a model sugar showed that exchange rates at pH < 5 are negligible.[31]

A second problem in quantitative interpretation of amide proton NOESY data arises from the use of frequency-selective pulses for solvent suppression. The intensity profile generated by the 1-1 echo read pulse in the NOESY experiment depends on the relationship $\sin \omega\tau_1 [(1 - \cos \omega\tau_2)/2]$ where τ_1 and τ_2 are delays in the excitation and refocusing pulses, respectively. In our experiments, $\tau_2 = 2\tau_1$ such that excitation was maximum at the NH resonance which was approximately 1800 Hz from the carrier (H_2O) frequency. Although relative intensities of peaks in columns of the spectrum are not affected by the 1-1 echo read pulse, intensities in rows of the spectrum need to be scaled by the factor $\sin^3 \pi\omega/2\omega_m$ where ω is the resonance offset from the carrier frequency and ω_m is the frequency at which excitation is maximum.[18] In our measurements in water we have used only columns of spectra, eliminating the need for this scaling factor. In this case, normalization was done by integrating the NH proton diagonal peak in a column and extrapolating to zero mixing time with its selective T_1 to determine its intensity at $t_m = 0$. Any crosspeak in this column could now be normalized with this value.

A third class of problems in the quantitative interpretation of amide proton NOEs results from its attachment to an ^{14}N nucleus which possesses both a magnetic dipole and electric quadrupole moment providing several relaxation mechanisms. Scalar relaxation modulated by chemical exchange, which arises when one proton of a coupled pair is exchanging, is insignificant under our conditions of small coupling constants ($^3J_{NH-H_2} \approx 10$ Hz) and the relatively long exchange lifetimes for the amide proton. This type of relaxation becomes significant only when exchange lifetimes are of the order of 10^{-5} s or shorter and with large coupling constants.[32]

Rapid quadrupolar relaxation of the ^{14}N nucleus results in modulation of the ^{14}N-H spin-spin coupling which provides a scalar mechanism of the second kind for the proton attached to it.[33-35] The scalar coupling J_{N-H} contributes to the amide proton T_1 relaxation by[33,36]

$$\frac{1}{T_{1(H)}^{SC}} = \frac{8\pi^2 J^2 I_N(I_N + 1)}{3}\left(\frac{Tq_N}{1 + (\omega_H - \omega_N)^2 Tq_N^2}\right) \quad (1)$$

where ω_H and ω_N are Larmor frequencies of ^1H and ^{14}N, respectively. The ^{14}N quadrupolar relaxation rate Tq_N^{-1} can be calculated from[33,36]

$$Tq_N^{-1} = \frac{3}{80}\left(1 + \frac{\eta^2}{3}\right)\left(\frac{e^2qQ}{\hbar}\right)\left(\frac{2\tau_c}{1 + \omega^2\tau_c^2} + \frac{8\tau_c}{1 + 4\omega^2\tau_c^2}\right) \quad (2)$$

(30) Narutis, V. P.; Kopple, K. D. *Biochemistry* **1983**, *22*, 6233-6239.
(31) Huang, D. H.; Pritchard, D. G.; Sakai, T. T.; Krishna, N. R. *Biochem. Biophys. Res. Commun.* **1987**, *143*, 685-690.
(32) Glickson, J. D.; Gordon, S. L.; Pitner, T. P.; Agresti, D. G.; Walter, R. *Biochemistry* **1976**, *15*, 5721-5729.
(33) Abragam, A. *The Principles of Nuclear Magnetism*; Oxford University Press: London, 1961; pp 309-312.
(34) Kintzinger, J. P.; Lehn, J. M. *Mol. Phys.* **1968**, *14*, 133.
(35) Kumar, A.; Rama Krishna, N.; Nageswara Rao, B. D. *Mol. Phys.* **1970**, *18*, 11.
(36) Witanowski, M.; Webb, G. A. *Nitrogen NMR*; Plenum Press: New York, 1973; pp 134-139.

where η is the asymmetry parameter, $e^2qQ/\hbar$ is the electric quadrupolar coupling constant, and ω = 36.118 MHz × 2π. The coupling constant $J_{^{15}N-H}$ for amides, needed in eq 1, shows little variation with structure with values ranging from 88 to 92 Hz.[36] $J_{^{14}N-H}$ calculated from the known $J_{^{15}N-H}$ value for formamide and the ratio of the gyromagnetic ratios of ^{15}N and ^{14}N is ≈64 Hz. Other parameters needed for eq 2 include the asymmetry parameter (η) of 0.37 and $e^2qQ/\hbar$ of 2.274 *MHz* which were also taken from formamide. The ^{14}N quadrupolar relaxation rate Tq_N^{-1} depends on the correlation time τ_c for which a value of 1 ns, obtained by reproducing intraresidue NOEs in LND-1 and LNF-1, was used. With these values Tq_N is estimated to be 15 μs, and the contribution of T^{-1}_{SC} to the amide proton spin–lattice relaxation rate is negligible, $\approx 2 \times 10^{-9}$ s^{-1}. It is to be noted that although the scalar contribution to T_1 relaxation of the amide proton is small, the effect on T_2 relaxation can be significant.[36]

Dipolar relaxation of the amide proton originates from two kinds of interactions. The first interaction, which involves the amide proton and other protons in the molecule, is the more useful because it provides information on geometry. The second is dipolar interaction with the directly bonded ^{14}N nucleus, which depends mainly on the distance r_{N-H} and correlation time τ_c. Assuming an isotropic model, the dipolar relaxation rate R_1 of an amide proton interacting with another dipolar nucleus j with spin quantum number $I \geq {}^1/_2$ can be calculated from the equation[33,37-39]

$$R_1 = \frac{1}{T_1} = \frac{2}{15}\left(\frac{\mu_0}{4\pi}\right)^2 \hbar^2\gamma_H^2 \sum_j I_j(I_j + 1)\gamma_j^2 r_{ij}^{-6}\chi_j \qquad (3)$$

where

$$\chi_j = \frac{\tau_c}{1 + (\omega_j - \omega_H)^2\tau_c^2} + \frac{3\tau_c}{1 + \omega_H^2\tau_c^2} + \frac{6\tau_c}{1 + (\omega_j + \omega_H)^2\tau_c^2}$$

Due in part to the shorter ^{14}N–H distance and the fact that $I_j(I_j + 1) = 2$ for ^{14}N the contribution to dipolar relaxation of amide proton from directly bonded ^{14}N can be significant.[40] It has been found that for nonprotonated ^{13}C with a directly bonded ^{14}N the dipolar contribution to ^{13}C T_1 and the resulting effect on ^{13}C NOE intensities is substantial.[37,41] Incorporation of ^{14}N dipolar contribution significantly improves agreement between calculated and experimental results.[39,41] In our calculations this contribution to the overall amide T_1 was estimated to be 0.67 s^{-1} at 500 MHz (^1H), assuming an N–H distance of 1.0 Å and τ_c of 1 ns. This was added to the contribution from ^1H–^1H interactions which was calculated by using the same eq 3 and substituting the appropriate values of I, ω and r_{ij}. It was found that for the amide NOEs simulated (range ≈ 1–5%) incorporation of this contribution resulted in the calculated values being ≈0.6% less than those calculated without the ^{14}N–H contribution.

The above considerations provided for incorporation of NH NOESY crosspeaks into the simulations yielding additional information on the glycosidic dihedral angles as well as information regarding the relative orientation of the amide side chain in GlcNAc which had been deduced to be in a trans arrangement based on coupling constant measurements[3] and observations of NOEs from the methyl group of the acetamido side chain to neighboring protons Fuc[2] H3 and Gal[3] H1 in LND-1.[4,26] The contour plot and a cross section of the NOESY spectrum of LND-1 in H_2O at 250 ms mixing time (Figure 3) show NOEs from the NH proton of GlcNAc to protons within the same residue (GlcNAc H1, H2 and H3) and to a proton in an adjacent residue (Gal[3] H1). Although this latter resonance overlaps with β-Glc H1 in both LND-1 and LNF-1, our model building suggests that the β-Glc residue is at a considerable distance from the amide group making it unlikely for any of its protons to show NOE to the amide proton. NOESY experiments for LND-1 in mixtures of DMSO–H_2O, in which these two resonances are well-separated, showed that the amide NOE peak was to Gal[3] H1 and not to β-Glc H1. Simulation of NOEs from exchangeable protons were consistent with the glycosidic ψ and Φ angles derived by simulation of nonexchangeable proton NOEs providing additional support for our proposal of a single rigid conformation for LND-1 reported previously.[4] In conformational energy calculations previously carried out for disaccharide fragments modeling the type 1 and type 2 β-galactosyl linkage and in which the orientation of the amide plane of GlcNAc was explicitly included, several low-energy conformations for the amide dihedral angle τ were reported.[3] Two of these were found near the trans amide proton orientation (τ = 100° and 140°) and one at a cis orientation (τ = −60°). We rule out the cis orientation based on the large (J = 10.1 Hz) coupling constant observed. The two low-energy trans conformations differ in the proximity of the amide proton to H1 or H3 of GlcNAc. Since, at τ = 100° the amide proton is closer to H3 than to H1 whereas the opposite is true for τ = 140°, it is possible to distinguish between these two orientations from the calculated amide proton NOEs. The NOESY simulations showed that the conformation τ = 90° ± 20° (Table III) is consistent with the experimental data in which a larger NOE to H3 than to H1 is observed as well as a relatively large NOE to H1 of Gal[3].

As in LND-1, the contour plot and cross section of the NOESY spectrum of LNF-1 in 90% H_2O/10% D_2O at 250 ms (Figure 2) show crosspeaks to GlcNAc H3 and Gal[3] H1 from the amide proton and a small (<1%) effect to GlcNAc H2. Unlike in LND-1, no crosspeak to GlcNAc H1 was observed suggesting that there may be differences in the amide orientation in the two oligosaccharides. Simulation of these NH and carbon-bound proton NOEs obtained previously and comparison with experimental NOEs also resulted in a near-trans conformation of the NH proton relative to GlcNAc H2, with the value τ = 60° ± 30° (Table III) for the amide dihedral angle, a value which is slightly different from that found for LND-1. The amide proton was also found to be closer to H3 than to H1 of the GlcNAc residue, and the calculated NOE to H1 (GlcNAc) was <1%. We propose that this modest difference in the amide dihedral angles may explain the difference in the CD bands assigned to the amide chromophores of LNF-1 and LND-1 seen in Figure 4.

The NH NOE intensities for both LND-1 and LNF-1 under the conditions used were generally small, but these effects were reproducible and could be measured accurately to within ±1%. The wider range (50–70°) of values for the amide dihedral angle consistent with experiment compared to the dihedral angles ψ and Φ indicates that the NH crosspeak intensities are not very sensitive to changes in the amide dihedral angle τ. Since the effects of exchange and other mechanisms of relaxation on the NH NOE intensities have been considered in the simulations, the reduced sensitivity of the NOE to changes in the amide angle τ is mainly a result of geometry. It is, therefore, not possible with this method to determine whether or not a single conformation of the acetamido side chain exists. On the other hand, we can exclude certain conformations based on these NH intensities, i.e., NH is closer to H3 than to H1 of GlcNAc, so τ = 140° is excluded. Molecular dynamics simulations of LND-1 and LNF-1 fragments suggest the existence of a narrow range of conformations for the glycosidic angles ψ and Φ and that the amide angle τ fluctuates about regions which closely match those obtained from NOESY simulations.[42]

Observation of NOEs from labile protons provides additional experimental constraints useful in studying the three-dimensional structures of carbohydrates.[43] Nuclear Overhauser effects from the hydroxyl and acetamido protons in ganglioside GM1[44] and globoside[45] have been used to determine the conformation of the

(37) Oldfield, E.; Norton, R. S.; Allerhand, A. *J. Biol. Chem.* **1975**, *250*, 6368–6380.
(38) Neuhaus, D.; Williamson, M. P. *The Nuclear Overhauser Effect in Structural and Conformational Analysis*; VCH Publishers: New York, 1989; p 53.
(39) Krishna, N. R.; Agresti, D. G.; Glickson, J. D.; Walter, R. *Biophys. J.* **1978**, *24*, 791–814.
(40) Llinas, M.; Klein, M. P.; Wuthrich, K. *Biophys. J.* **1978**, *24*, 849–862.
(41) Norton, R. S.; Allerhand, A. *J. Am. Chem. Soc.* **1976**, *98*, 1007–1014.
(42) Mukhopadhyay, C.; Bush, C. A. Submitted for publication.
(43) Dabrowski, J.; Poppe, L. *J. Am. Chem. Soc.* **1989**, *111*, 1510–1511.
(44) Acquotti, D.; Poppe, L.; Dabrowski, J.; von der Lieth, C. W.; Sonnino, S.; Tettamanti, G. *J. Am. Chem. Soc.* **1990**, *112*, 7772–7778.
(45) Poppe, L.; von der Lieth, C. W.; Dabrowski, J. *J. Am. Chem. Soc.* **1990**, *112*, 7762–7771.

oligosaccharide portions of these molecules in Me_2SO and Me_2NCHO. In these studies, the amide side chain (in GalNAcβ(1→3)Gal) was found to exist in two conformations basically involving torsions about the trans arrangement (τ = 160° and 60°). In this report we have shown by comparing experimental and simulated NOEs from the NH proton that for the oligosaccharides LND-1 and LNF-1 only one of these two conformations agrees with experiment.

Low-Temperature, Cooperative Conformational Transition within [Zn-Cytochrome *c* Peroxidase, Cytochrome *c*] Complexes: Variation with Cytochrome

Judith M. Nocek,[†] Eric D. A. Stemp,[†] Michael G. Finnegan,[‡] Thomas I. Koshy,[§] Michael K. Johnson,[‡] E. Margoliash,[§] A. Grant Mauk,[⊥] Michael Smith,[⊥] and Brian M. Hoffman*,[†]

Contribution from the Departments of Chemistry and Biochemistry, Molecular Biology, and Cell Biology, Northwestern University, Evanston, Illinois 60208, Department of Chemistry, University of Georgia, Athens, Georgia 30602, and Department of Biochemistry, University of British Columbia, Vancouver, British Columbia, Canada V6T 1Z3. *Received January 7, 1991*

Abstract: Conformational dynamics within the complex between Zn-substituted cytochrome *c* peroxidase (ZnC*c*P) and cytochrome *c* (C*c*) has been studied by examining the quenching of the ^{3}ZnP excited state by the ferriheme of C*c*. The temperature and solvent dependence of the triplet-state quenching rate constants (k_q) show that complexes of ZnC*c*P with a large set of Fe^{3+} cytochromes *c* undergo a transition between a low-temperature state that does not exhibit triplet quenching and a high-temperature state that does. Within the narrow transition range (220 K < *T* < 250 K), the decay traces for the [ZnC*c*P, Fe^{3+}C*c*] complexes are nonexponential, and outside of this range they are exponential. This behavior is displayed by complexes with C*c*(*Drosophila melanogaster*), C*c*(*Candida krusei*) and a suite of site-directed mutants of C*c*(yeast iso-1) where position 82 contains either an aliphatic (Met, Ser, Leu, or Ile) or an aromatic (Phe) residue. Above 250 K, k_q varies strongly among these complexes and decreases sharply with the concentration of cosolvent (EG = ethylene glycol), apparently because of increasing viscosity, while both the breadth of the transition range and its midpoint vary little within this class. MCD and optical spectra between ambient and 4 K rule out the trivial explanation that the transition might reflect changes in the coordination state, and the invariance of k_q with a 10-fold increase in [C*c*] shows that the proteins remain bound as a complex upon cooling. As the midpoint and breadth of the transition are unaffected by changes in percent EG, the transition does not appear to arise from a solvent-driven process. Instead, we propose that, at ambient temperatures, the binding interface of the [C*c*P, C*c*] complex undergoes rapid dynamic rearrangements between the subset of conformers that exhibit ^{3}ZnP quenching and the subset that does not. Below the transition range, the complex exists in the latter form, and it is suggested that, upon heating, there is a cooperative loosening of the binding interactions within the interface. We present an heuristic description of the complex based on the statistical mechanical description of the cooperative helix-coil transition in poly(amino acids). In contrast, members of a second class of complexes, those with C*c*(horse), C*c*(tuna), and C*c*(rat), have low quenching rate constants ($k_q \approx 40\ s^{-1}$ at ambient) that decrease smoothly to $k_q \approx 0\ s^{-1}$ by 250 K. Furthermore, k_q for these complexes shows little dependence upon either solvent or cytochrome, and the triplet decay traces remain exponential at all temperatures.

Introduction

In this paper, conformational dynamics within the complex between Zn-substituted cytochrome *c* peroxidase (ZnC*c*P) and cytochrome *c* (C*c*) has been studied by examining the quenching of the ^{3}ZnP excited state by the ferriheme of C*c*.[1-3] This complex is particularly well suited for such studies for several reasons. At low ionic strengths, the complex forms with a large protein association constant ($K_a = 10^7\ M^{-1}$)[4] and a model for the physiological complex has been generated[5] from the crystal structures of Fe^{3+}C*c*(tuna) and Fe^{3+}C*c*P from *Saccharomyces cerevisiae*. In addition, cytochromes *c* from numerous species, as well as site-directed mutants of both C*c* and C*c*P provide a wealth of complexes with which to probe the effects of structure on protein dynamics.[6,7]

In the proposed model for the [Fe^{3+}C*c*P, Fe^{3+}C*c*(tuna)] complex, generated by optimizing the electrostatic interactions between complementary surface charges on the two proteins, the complex is held together by electrostatic interactions between positively charged residues near the exposed heme crevice of C*c* (Lys 13, 27, 72, 86, and 87) and negatively charged residues on the surface

[†] Department of Chemistry, Northwestern University.
[‡] Department of Chemistry, University of Georgia.
[§] Department of Biochemistry, Molecular Biology, and Cell Biology, Northwestern University.
[⊥] Department of Biochemistry, University of British Columbia.

(1) Examples of conformational gating within hemoproteins include (a) Yuan, X.; Songcheng, S.; Hawkridge, F. M. *J. Am. Chem. Soc.* **1990**, *112*, 5380-5381. (b) Isied, S. S. In *Electron Transfer in Biology and the Solid State*; Johnson, M. K., et al., Eds.; American Chemical Society: Washington, DC, 1990; pp 91-100.
(2) Examples of conformational gating within electrostatic complexes include (a) Peerey, L. M.; Kostic, N. *Biochemistry* **1989**, *28*, 1861-1868. (b) Morand, L. Z.; Frame, M. K.; Colvert, K. K.; Johnson, D. A.; Krogmann, D. W.; Davis, D. J. *Biochemistry* **1989**, *28*, 8039-8047. (c) Pan, L. P.; Frame, M.; Durham, B.; Davis, D.; Millet, F. *Biochemistry* **1990**, *29*, 3231-3236.
(3) Examples of conformational gating within [C*c*P, C*c*] complexes include (a) Hazzard, J. T.; Poulos, T. L.; Tollin, G. *Biochemistry* **1987**, *26*, 2836-2848. (b) Cheung, E.; English, A. M. *Inorg. Chem.* **1988**, *27*, 1078-1081.
(4) (a) Erman, J. E.; Vitello, L. B. *J. Biol. Chem.* **1980**, *255*, 6224-6227. (b) Nicholls, P.; Mochan, E. *Biochem. J.* **1971**, *121*, 66-67. (c) Mochan, E.; Nicholls, P. *Biochim. Biophys. Acta* **1972**, *267*, 309-319. (d) Vitello, L. B.; Erman, J. E. *Arch. Biochem. Biophys.* **1987**, *258*, 621-629.
(5) Poulos, T. L.; Kraut, J. *J. Biol. Chem.* **1980**, *255*, 10322-10330.
(6) Liang, N.; Mauk, A. G.; Pielak, G. J.; Johnson, J. A.; Smith, M.; Hoffman, B. M. *Science* **1988**, *240*, 311-313.
(7) Ho, P. S.; Sutoris, C.; Liang, N.; Margoliash, E.; Hoffman, B. M. *J. Am. Chem. Soc.* **1985**, *107*, 1070-1071.

0002-7863/91/1513-6822$02.50/0